Electromechanical coupling in nonpiezoelectric materials due to nanoscale nonlocal size effects: Green's function solutions and embedded inclusions

R. Maranganti,[1] N. D. Sharma,[1] and P. Sharma[1,2,*]

[1]*Department of Mechanical Engineering, University of Houston, Houston, Texas 77204, USA*

[2]*Department of Physics, University of Houston, Houston, Texas 77204, USA*

In a piezoelectric material, an applied *uniform* strain can induce an electric polarization (or vice versa). Crystallographic considerations restrict this technologically important property to noncentrosymmetric systems. It has been shown both mathematically and physically that a *nonuniform* strain can potentially break the inversion symmetry and induce polarization in nonpiezoelectric materials. The coupling between strain gradients and polarization, and conversely between strain and polarization gradients, is investigated in this work. While the conventional piezoelectric property is nonzero only for certain select materials, the nonlocal coupling of strain and electric field gradients is (in principle) nonzero for all dielectrics, albeit manifesting noticeably only at the nanoscale, around interfaces or in general in the vicinity of high field gradients. Based on a field theoretic framework accounting for this phenomena, we (i) develop the fundamental solutions (Green's functions) for the governing equations, and (ii) motivated by eventual applications for quantum dots, solve the general embedded mismatched inclusion problem with explicit results for the spherical and cylindrical shape. Expectedly, our results for the aforementioned problems are size dependent and indicate generation of high electric fields reaching values of approximately hundreds of kV/m in selected sizes and locations—even in isotropic centrosymmetric nonpiezoelectric materials.

PACS number(s): 77.65.−j

I. INTRODUCTION AND BACKGROUND

In the traditional continuum field theory of piezoelectric materials, an electric polarization is generated in response to uniform strain (or vice versa). Within the assumptions of linearity, a third-rank piezoelectric tensor **p** relates the polarization vector **P** to the second-rank strain tensor **e**,[1]

$$P_i = p_{ijk}e_{jk}. \tag{1}$$

Crystallographic considerations restrict this technologically important property to noncentrosymmetric crystal systems and, indeed, the latter is a necessary condition for a material to exhibit piezoelectricity (e.g., GaN and ZnO are piezoelectric but Si and NaCl are not). Figure 1 provides an illustration of piezoelectricity based on the crystal structure of ZnO.

Tensor transformation properties require that under inversion-center symmetry, all odd-order tensors vanish. Thus, most common dielectrics are not piezoelectric. Physically, however, it is easy to visualize how a *nonuniform strain* could potentially break the inversion symmetry and induce polarization. This is tantamount to extending relation (1) to include strain gradients

$$P_i = \underbrace{p_{ijk}\varepsilon_{jk}}_{=0,\text{for nonpiezo materials}} + \mu_{ijkl}\frac{\partial^2 u_j}{\partial x_k \partial x_l}. \tag{2}$$

In some circles; this particular electromechanical coupling is known as the "flexoelectric effect" (e.g., Tagantsev[2]) and the components of the tensor **μ** are the so-called flexoelectric coefficients. While the piezoelectric property is nonzero only for certain select materials, the strain gradient-polarization coupling (i.e., flexoelectric coefficients) are in principle nonzero for all dielectrics including the isotropic continuum.

This implies that under a nonuniform strain, all dielectrics are capable of producing a polarization. One may extend similar arguments to link polarization gradients to the strain tensor through a converse effect, i.e., reverse flexoelectricity. The latter, for example, has been the focus of work of Mindlin[3] who introduced an extended nonlocal theory of piezoelectricity by incorporating coupling of polarization gradients to strain. Figure 2 illustrates how NaCl (which is nonpiezoelectric) will yield zero net dipole moment (and hence no polarization) under application of uniform strain but will exhibit an apparent piezoelectric effect when subjected to strain gradients, e.g., bending or inhomogeneous stretching.
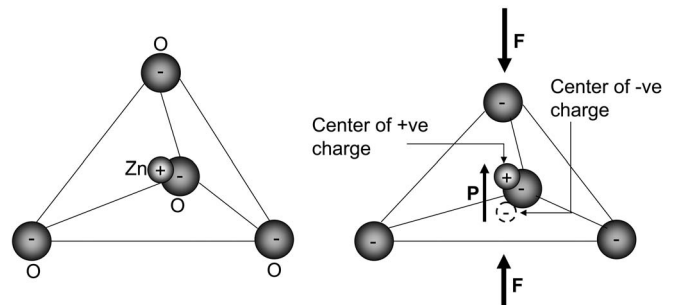

FIG. 1. Illustration of "classical" piezoelectricity. The left figure shows the tetrahedrally coordinated cation-anion unit of a ZnO crystal. The center of negative charge of the oxygen (O) anions coincides with the center of positive charge which is located at the zinc (Zn) ion. Thus, there is no net dipole polarization in the absence of external pressure. Upon application of external pressure, the centers of positive and negative charge suffer relative displacement with respect to each other, thereby inducing a dipole moment. Such dipole moments are induced throughout the crystal lattice, thereby giving rise to net polarization.
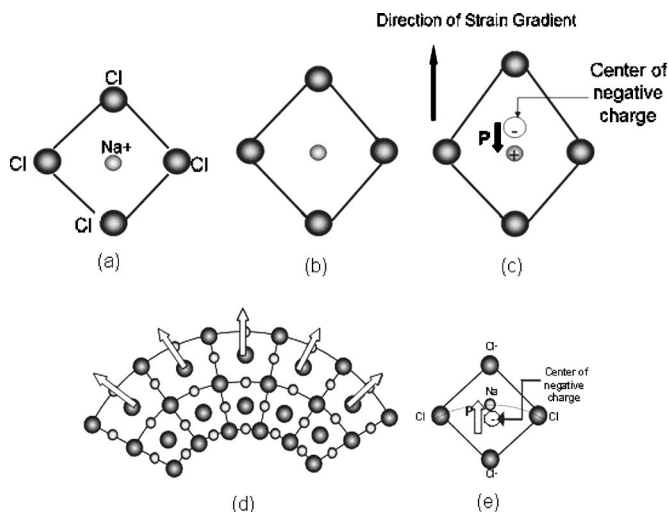
FIG. 2. (a) Undeformed NaCl unit cell. The sodium ion is positively charged while the four neighboring chlorine ions are negatively charged. As can be seen, the centers of gravity of the negative charge and the positive charge coincide leading to (expectedly) zero net dipole moment. (b) Uniform strain. Application of a uniform strain displaces all ions by the same distance and hence the centers of gravity of the negative and positive charges coincide again, thereby resulting in zero net polarization—implying that NaCl is nonpiezoelectric. The final positions of the ions are shown in dark while the initial positions are shown in pale. (c) NaCl unit cell under nonuniform stretching. Application of a nonuniform strain, however, results in relative displacement of the centers of the negative charge and positive charge with respect to each other. This results in a dipole moment (represented by the thick red arrow) in the direction opposite to the strain gradient for the considered cell. (d) and (e) polarization due to bending.

What is the magnitude of this effect? Both common sense and (soon to be discussed) experimental evidence indicate that this effect is very small unless large strain or electric field gradients are present. Consider a structure with certain mechanical boundary conditions; the mechanical strain can be considered to be roughly the same if the system is shrunk self-similarly from mm's to nm's.[4] However, the strain gradient will increase by six orders of magnitude. For example, in the case of a NaCl plate, at 10 nm thickness, the electromechanical coupling factor[5] [Vibration response under applied alternating voltage. Obviously since NaCl is nonpiezoelectric, one would expect the electromechanical factor to be zero unless the flexoelectric effects (or its converse) are accounted for.] reaches 80% of the value of quartz or alternatively 12% of the piezoelectric transducer (PZT). As will be discussed in due course, the size dependency of electric fields in embedded strain-mismatched inclusions (such as quantum dots) is somewhat richer and more complex. Close to interfaces and surfaces, electric fields in the neighborhood of 10^5 V/m may be expected (e.g., see our results in Sec. V and the one-dimensional examples in Mindlin[3] and Nowacki[6]).

While not quite widely known in the crystalline solids community, this phenomenon has been experimentally observed in a variety of contexts: bending of crystal plates (e.g., Bursian and Trunov[7]) and measurements on thin films.[8]

It has also been used to explain the anomalous capacitance measurements of thin dielectric films,[9] may be employed to explain the weak piezoelectric behavior of carbon nanotubes,[10] and provides an explanation for the size-dependent piezoelectric behavior of boron nitride nanotubes.[11] An interesting experimental manifestation of the flexoelectric effect is in dislocated diatomic crystals. Overall macroscopic electromechanical effects of otherwise nonpiezoelectric crystals have been attributed to polarization in the vicinities of dislocations.[12–15] The aforementioned works are related to crystalline materials. As an aside, we note here that a large literature also exists in the liquid crystal and biological membrane context which, however, is not of interest in the present work. It is noteworthy, though, that the term "flexoelectricity" for crystalline materials was coined inspired by similar phenomenon in liquid crystals.[16–18]

A crude analysis to measure the magnitude of the flexoelectric coefficients was first provided by Kogan[19] who estimated the coefficients to be of the order of e/a, where e is the electronic charge and a is lattice parameter. Multiplication by relative permittivity for normal dielectrics was suggested,[19] which now appears to have been confirmed experimentally.[20] Marvan and Havranek[21] studied the flexoelectric effect via a simple linear chain model of ions and arrived at a similar estimate. Of course, the flexoelectric effect also exists in classically piezoelectric materials and may provide large corrections to electric field or strain calculations for problems involving small length scales (e.g., Nowacki[6]). Experimental measurements of the flexoelectric effect on ceramics such as lead magnesium niobate, barium strontium titanate, and lead zirconate titanate[20,22,23] show that the magnitude of their flexoelectric coefficients is of the order of 10^{-6} C/m, which is much larger than the generally accepted lower bound of e/a ($\approx 10^{-9}$ C/m).

From a theoretical standpoint, two distinct bodies of works appear to have emerged that, while quite related, have apparently been developed independently. The pioneering work within the mechanics of materials community is due to Mindlin.[3] Lattice level "shell" type models of crystalline dielectrics clearly indicate that the long wavelength limit of the lattice dynamical results do not lead to the classical piezoelectric theory. The latter, from an atomistic point of view, is simply the long wavelength representation of the core-core interactions while core-shell and shell-shell interactions are neglected.[24–26] "Inspired" by this discrepancy, Mindlin[3] introduced a continuum field theory that incorporates coupling of polarization gradients to strain (or, in our language, the reverse flexoelectric effect). It is found that such a theory does indeed correctly represent, within a continuum field-theoretic formalism, the core-shell and shell-shell interactions (see also the study of Askar *et al.*[27]). We point out that Mindlin's theory does not incorporate the direct flexoelectric effect or the strain gradient-polarization coupling discussed earlier. Several works subsequently appeared that expanded on Mindlin's original theory. For example, Mindlin himself showed that his formulation could be used to explain the anomalous capacitance behavior of thin films.[9] Askar *et al.*[28] considered elastic and dielectric states of cylindrical and spherical cavities as well as cracks. In a later paper, using lattice dynamical methods, the same authors also evaluated

the material constants of Mindlin's theory for KCl and NaCl.[29] The Green's functions for Mindlin's restricted theory were derived by Nowacki and Glockner.[30] Two remarkable features emerge from Mindlin's theory. It was found capable to take into account surface energy (without increasing the order of the governing differential equations) and predicted a piezoelectric coupling even in isotropic continua.

In parallel, essentially the same subject has been discussed from arguably a different perspective in the condensed matter physics literature. Inspired by the experimental observations already discussed earlier, a phenomenological description of the flexoelectric effect was proposed.[19] Based on microscopic considerations, several concepts related to flexoelectricity and classical piezoelectricity were clarified.[2] Later, Tagantsev critically reviewed the literature and further expounded on the phenomenological description of flexoelectricity.[31] The relation of crystal structure to flexoelectricity was discussed[17] and a simple lattice-spring type model that provides formulae for computation of the flexoelectric coefficients has been proposed.[21] Further, the reader may refer to Maugin's book[32] where the classification of various types of electromechanical couplings has been comprehensively documented in addition to several instructive examples. Yet another electromechanical coupling effect which deserves mention is the phenomena of electrostriction.[32] Like flexoelectricity, this phenomenon is also universal to all dielectrics (including centrosymmetric ones); however, this is where the similarity ends. In electrostriction, the strain depends on the square of the electric field. Thus, an applied electric field can produce a deformation due to this nonlinear coupling. A converse effect does not exist and, because of the square dependence, reversal in an electrical field direction does not cause a reversal in deformation. Typical electrostriction coefficients indicate that very high fields are required to manifest this effect. In contrast, flexoelectricity is more similar to piezoelectricity (i.e., it is a two-way coupling), shows strain reversal with polarization reversal, and is exhibited even at small strain levels (provided of course that the gradients are large enough as for instance in nanostructures).

In the present work, we tackle the following problems:

(i) Derivation of the Green's functions for the governing equations of an isotropic centrosymmetric continuum medium that incorporates *the flexoelectric effect, its converse, and the purely elastic nonlocal strain gradient effects*.

(ii) Predicated on the developed Green's function, the elastic and electric fields solution to the strain-mismatched embedded inclusion problem with explicit results for the spherical and cylindrical shape.

The motivation for developing Green's function hardly needs any emphasis. The determination of the latter provides an elegant framework for a variety of problems including the ones included the present work, e.g., the embedded inclusion problem and that of defects. The inclusion problem is itself of fair amount of interest. The classical linear elastic solution of strain mismatched inclusion due to Eshelby[33] has a distinguished place in the history of materials science, mechanics, and solid-state physics. Eshelby's solution of the embedded inclusion has been fruitfully used in diverse areas and problems of physical sciences, e.g., localized thermal heating,

phase transformations, overall or effective properties of composites, quantum dots, and microstructural evolution, to name just a few. In particular, quantum dots are essentially nanoinclusions subjected to lattice mismatch transformation strains that, due to the flexoelectric effect, may be subjected to high electric fields. The latter, in turn, can significantly impact the optoelectronic properties of quantum dots through the so-called Stark effect.[34] Within the classical piezoelectric theory also, the electromechanical coupling in embedded inclusions and quantum dots has attracted fair attention (see, for example, Pan,[35,36] Li and Dunn,[37] and the review article by Maranganti and Sharma[38]).

The outline of our paper is as follows. In Sec. II, the general formulation for a flexoelectric medium is given in a systematic manner. The governing equations are derived based on a physically consistent Lagrangian. The fundamental solutions of the governing equations are derived in Sec. III while the general inclusion problem is formulated in Sec. IV. We focus on the inclusion solution to the spherical and cylindrical shape in Sec. V, where closed form expressions are given. We finally conclude with a summary and our major conclusions in Sec. VI.

II. GENERAL FORMULATION

Although different in some respects, our presentation of the formulation and the governing equations parallel those of Sahin and Dost.[39] The difference when compared with Mindlin's framework lies in our inclusion of the flexoelectric coupling as well as purely elastic nonlocal terms. Within the assumption of an extended linear theory for *centrosymmetric* dielectrics incorporating terms involving first gradients of the deformation gradient and the polarization, the most general expression for the internal energy density function Σ, can be written as

$$\Sigma = \frac{1}{2}a_{kl}P_kP_l + \frac{1}{2}b_{ijkl}P_{i,j}P_{k,l} + \frac{1}{2}c_{ijkl}e_{ij}e_{kl} + d_{ijkl}P_{i,j}e_{kl}$$

$$+ f_{ijkl}P_iu_{j,kl} + \frac{1}{2}g_{ijklm}u_{i,jk}u_{l,mn}. \tag{3}$$

Here, **u** and **P** are the displacement and the polarization vectors respectively, while the comma denotes differentiation with respect to the spatial variables.

Additionally, e_{ij} are the components of the strain tensor **e** defined as usual,

$$e_{ij} = \frac{1}{2}(u_{i,j} + u_{j,i}), \tag{4}$$

where **a**, **b**, **c**, **d**, **f**, and **g** are material property tensors. In particular, **a** and **c** are the familiar second-order reciprocal dielectric susceptibility and fourth-order elastic constant tensors, respectively. The remaining tensors correspond to higher order electroelastic couplings which do not occur in the classical continuum description of an isotropic elastic dielectric. **d**, which was introduced by Mindlin[3] in his theory of polarization gradient, links gradients of polarization to strains while the components of **f** are the flexoelectric coef-

ficients. It should be noted that while the tensors **f** and **μ** [from Eq. (2)] can both be addressed as "flexoelectric coefficients," the former represents the coupling between the electric field and the gradient of strain while the latter links the polarization to the gradient of the strain. The tensor **g** represents purely nonlocal elastic effects and corresponds to the so-called strain gradient elasticity theories. Note that all the tensors corresponding to the material properties are of even order since the restriction to centrosymmetry (i.e., classically nonpiezoelectric materials) requires that odd tensors vanish.

The internal energy density of Eq. (3) is invariant under the Euclidean group $SO(3) \triangleright T(3)$ i.e., the semi-direct product of the rigid rotation group $SO(3)$ and the rigid translation group $T(3)$. Invariance under rigid translations ensures that the internal energy density can only depend upon the first and higher order derivatives of the displacement, $\nabla \otimes \nabla \otimes \cdots \mathbf{u}$ and not on the displacement **u** itself. Invariance restrictions under rigid rotations only permit the symmetric part of the displacement gradient [given by the strain tensor of Eq. (4)], to contribute to the internal energy density expression. However, starting from the second derivative, all higher derivatives of the displacement vector, i.e., $\nabla \otimes \nabla \otimes \cdots \mathbf{u}$, transform properly under $SO(3) \triangleright T(3)$. The invariance restrictions do not manifest themselves in relation to the polarization vector **P** and the internal energy density is allowed to depend on polarization as well as all its higher-order derivatives.

The symmetries of the material constants introduced in Eq. (3) have been investigated. The symmetry properties of the elastic moduli tensor **c** are of course well known.[1] For **b** and **d**, refer to Mindlin[9] while Kogan[19] may be consulted for the flexoelectric tensor **f**. The reductions are listed below, as follows:

$$a_{ij} = a\delta_{ij},$$

$$c_{ijkl} = (c_{11} - c_{12} - 2c_{44})\delta_{ijkl} + c_{12}\delta_{kl} + c_{44}(\delta_{ik}\delta_{jl} + \delta_{il}\delta_{jk}),$$

$$b_{ijkl} = (b_{11} - b_{12} - 2b_{44})\delta_{ijkl} + b_{12}\delta_{kl} + b_{44}(\delta_{ik}\delta_{jl} + \delta_{il}\delta_{jk}) + b_{77}(\delta_{ik}\delta_{jl} - \delta_{il}\delta_{jk}),$$

$$d_{ijkl} = (d_{11} - d_{12} - 2d_{44})\delta_{ijkl} + d_{12}\delta_{kl} + d_{44}(\delta_{ik}\delta_{jl} + \delta_{il}\delta_{jk}),$$

$$f_{ijkl} = (f_{11} - f_{12} - 2f_{44})\delta_{ijkl} + f_{12}\delta_{kl} + f_{44}(\delta_{ik}\delta_{jl} + \delta_{il}\delta_{jk}). \tag{5}$$

Under conditions of isotropy, the following constraint holds

$$\alpha_{11} - \alpha_{12} - 2\alpha_{44} = 0 \quad \text{where } \alpha = b, c, d, f. \tag{6}$$

Thus for isotropic space, Eqs. (6) simplify further to

$$a_{ij} = a\delta_{ij}, \quad c_{ijkl} = c_{12}\delta_{kl} + c_{44}(\delta_{ik}\delta_{jl} + \delta_{il}\delta_{jk}),$$

$$b_{ijkl} = b_{12}\delta_{kl} + b_{44}(\delta_{ik}\delta_{jl} + \delta_{il}\delta_{jk}) + b_{77}(\delta_{ik}\delta_{jl} - \delta_{il}\delta_{jk}),$$

$$d_{ijkl} = d_{12}\delta_{kl} + d_{44}(\delta_{ik}\delta_{jl} + \delta_{il}\delta_{jk}),$$

$$f_{ijkl} = f_{12}\delta_{kl} + f_{44}(\delta_{ik}\delta_{jl} + \delta_{il}\delta_{jk}). \tag{7}$$

The nonlocal elasticity tensor **g** is associated with pure elastic strain gradient terms. Several treatments exist in the literature to include pure strain gradient effects in the internal energy, e.g., Kleinert.[40] The contributions of purely elastic strain gradient terms to the internal energy as Σ^K can be expressed as

$$\Sigma^K = \frac{1}{2}c_{11}l'^2 \partial_i \partial_l u_l \partial_i \partial_j u_j + \frac{1}{2}c_{44}l^2(\partial_l^2 u_i \partial_l^2 u_i - \partial_i \partial_l u_l \partial_i \partial_j u_j), \tag{8}$$

l' and l are two new material constants having the dimensions of length. While l' provides a higher order correction to the dilation field, l characterizes resistances to gradients of rotation (see also, Zhang and Sharma[41,42]). Comparison of Eqs. (8) and the last term on the right-hand side of Eq. (3) make evident the following reduction for the tensor g_{ijklmn}:

$$g_{ijklmn} = c_{11}l'^2 \delta_{ij}\delta_{kn}\delta_{lm} + c_{44}l^2(\delta_{il}\delta_{jk}\delta_{mn} - \delta_{ij}\delta_{kn}\delta_{lm}). \tag{9}$$

Standard variational analysis may now be employed to obtain a system of equilibrium equations, boundary conditions, and constitutive relations for an isotropic material occupying domain Ω and bounded by a surface S. We omit these details as such deductions are now routine in mechanics. The major variables, i.e., the electromechanical "stresses" are defined through the following relations:

$$t_{ij} \equiv \frac{\partial \Sigma}{\partial e_{ij}}, \quad t_{ijm} \equiv \frac{\partial \Sigma}{\partial u_{i,jm}},$$

$$E_{ij} \equiv \frac{\partial \Sigma}{\partial P_{i,j}}, \quad E_i \equiv \frac{\partial \Sigma}{\partial P_i}. \tag{10}$$

Notice that the definition of t_{ij} is the same as that of the stress tensor in classical elasticity; E_i is the effective local electric force. The terms t_{ijm} and E_{ij} can be thought of as higher order stress (moment stress) and higher order local electric force respectively. We now proceed to list the balance laws, boundary conditions, and the constitutive relations.

(i) The balance laws:

$$(t_{ij} - t_{jim,m})_{,j} + F_i = 0, \tag{11a}$$

$$E_{ij,j} + E_i - \phi_{,i} + E_i^0 = 0, \tag{11b}$$

$$-\varepsilon_0 \phi_{,ii} + P_{i,i} = 0 \quad \text{in } \Omega, \tag{11c}$$

$$\phi_{,ii} = 0 \quad \text{in } \Omega^*. \tag{11d}$$

In Eqs. (11a)–(11d), **F** and $\mathbf{E}^0$ are the external body force and electric field respectively while ϕ is the potential of the Maxwell self-field $\mathbf{E}^{MS}$, i.e.,

$$E_i^{MS} = -\phi_{,i} \tag{12}$$

In the absence of the higher order stress t_{ijm} which includes higher order gradients of the displacement vector (such as $u_{i,jm}$), Eq. (11a) reduces to the standard force balance equation of classical elasticity,

$$t_{ij,j} + F_i = 0. \tag{13}$$

Since the term $t_{ij} - t_{ijm,m}$ occurs in a force balance relation as evident in Eq. (11a), we may interpret it as a "physical stress," σ^{phys},

$$\sigma_{ij}^{phys} = t_{ij} - t_{ijm,m}. \tag{14}$$

Unlike the stress tensor in classical elasticity, the physical stress σ^{phys} of Eq. (14) is not symmetric. In particular, the lack of symmetry manifests due to the term $t_{ijm,m}$, which incorporates rotational effects.

(ii) The boundary conditions: For all $x \in S$, the following conditions hold:

$$n_i \sigma_{ij}^{phys} = t_j, \tag{15a}$$

$$n_i E_{ij} = 0, \tag{15b}$$

$$n_i(\llbracket \varepsilon_0 \phi_{,i} \rrbracket + P_i) = 0, \tag{15c}$$

where **n** and **t** are the exterior normal unit vector and the surface traction vector respectively; ε_0 is the dielectric constant, and the symbol $\llbracket \ \rrbracket$ denotes the jump across the surface S.

(iii) The constitutive relations:

$$t_{ij} = [c_{12}\delta_{ij}\delta_{ps} + 2c_{44}\delta_{ip}\delta_{js}]e_{ps}$$
$$+ [d_{12}\delta_{ij}\delta_{ps} + d_{44}(\delta_{is}\delta_{jp} + \delta_{js}\delta_{ip})]P_{p,s}, \tag{16a}$$

$$t_{ijm,m} = [(c_{12} + 2c_{44})l'^2\nabla^2\delta_{ij}\delta_{ps}]u_{p,s} + [f_{12}\delta_{pi}\delta_{js} + f_{44}(\delta_{ps}\delta_{ji} + \delta_{is}\delta_{jp})]P_{p,s} + c_{44}l^2\nabla^2(\delta_{is}\delta_{jp} - \delta_{js}\delta_{ip})u_{p,s}, \tag{16b}$$

$$E_{ij} = [d_{12}\delta_{ij}\delta_{ps} + d_{44}(\delta_{is}\delta_{jp} + \delta_{js}\delta_{ip})]u_{p,s} + [b_{12}\delta_{ij}\delta_{ps} + (b_{44} + b_{77})\delta_{is}\delta_{jp} + (b_{44} - b_{77})\delta_{js}\delta_{ip}]P_{p,s}, \tag{16c}$$

$$E_i = -\{aP_i + [f_{12}\delta_{ij}\delta_{ps} + f_{44}(\delta_{is}\delta_{jp} + \delta_{js}\delta_{ip})]u_{j,ps}\}. \tag{16d}$$

Notice that the last term in the expression for t_{ijm} [Eq. (16b)] is antisymmetric in the indices i and j, while the rest of the terms are symmetric. Thus a combination of symmetric and antisymmetric terms occur in the expression for the physical stress, σ^{phys}, which leaves it devoid of the familiar symmetry properties one associates with the classical stress tensor.

Substituting the constitutive relations (16a)–(16d) into the balance laws (11a)–(11d) yields the Navier-like equations for dielectrics in our extended theory that incorporates the flexoelectric effect, its converse, and the purely nonlocal elastic terms:

$$c_{44}\nabla^2\mathbf{u} + (c_{12} + c_{44})\nabla\nabla\cdot\mathbf{u} - (c_{12} + 2c_{44})l'^2\nabla^2\nabla\nabla\cdot\mathbf{u}$$
$$- c_{44}l^2(\nabla^2\nabla^2\mathbf{u} - \nabla^2\nabla\nabla\cdot\mathbf{u}) + (d_{44} - f_{12})\nabla^2\mathbf{P} + (d_{12}$$
$$+ d_{44} - 2f_{44})\nabla\nabla\cdot\mathbf{P} + \mathbf{F} = 0, \tag{17a}$$

$$(d_{44} - f_{12})\nabla^2\mathbf{u} + (d_{12} + d_{44} - 2f_{44})\nabla\nabla\cdot\mathbf{u} + (b_{44} + b_{77})\nabla^2\mathbf{P}$$
$$+ (b_{12} + b_{44} - b_{77})\nabla\nabla\cdot\mathbf{P} - a\mathbf{P} - \nabla\phi + \mathbf{E}^0 = 0, \tag{17b}$$

$$-\varepsilon_0\nabla^2\phi + \nabla\cdot\mathbf{P} = 0. \tag{17c}$$

III. DERIVATION OF THE FUNDAMENTAL SOLUTIONS (GREEN'S FUNCTIONS)

Equations (17a)–(17c) may be rewritten in an alternative form,

$$C_{ij}u_j + D_{ij}P_j + F_i = 0, \tag{18a}$$

$$D_{ij}u_j + B_{ij}P_j - \phi_{,i} + E_i^0 = 0, \tag{18b}$$

$$-\varepsilon_0\phi_{,ii} + P_{i,i} = 0. \tag{18c}$$

Here we have defined the following tensor operators:

$$C_{ji} = C_{jpis}\nabla_p\nabla_s = [c_{12}\delta_{jp}\delta_{is} + c_{44}(\delta_{ps}\delta_{ij} + \delta_{js}\delta_{ip}) - (c_{12} + 2c_{44})l'^2\delta_{jp}\delta_{is}\nabla^2 + c_{44}l^2(\delta_{ps}\delta_{ij} - \delta_{js}\delta_{ip})]\nabla_p\nabla_s, \tag{19a}$$

$$D_{ji} = D_{jpis}\nabla_p\nabla_s = [(d_{12} + d_{44} - 2f_{44})\delta_{jp}\delta_{is} + (d_{44} - f_{12})\delta_{ps}\delta_{ij}]\nabla_p\nabla_s, \tag{19b}$$

$$B_{ji} = B_{jpis}\nabla_p\nabla_s - a\delta_{ij} = [b_{12}\delta_{jp}\delta_{is} + (b_{44} + b_{77})\delta_{ps}\delta_{ij} + (b_{44} - b_{77})\delta_{js}\delta_{ip}]\nabla_p\nabla_s - a\delta_{ij}. \tag{19c}$$

We can define two sets of Green's functions $\{{}^fG_{in}, {}^f\Pi_{in}, {}^f\phi_n\}$ and $\{{}^EG_{in}, {}^E\Pi_{in}, {}^E\phi_n\}$ corresponding to Eqs. (18a)–(18c) as follows:

$$C_{ji}{}^fG_{in}(\mathbf{x} - \mathbf{x}') + D_{ji}{}^f\Pi_{in}(\mathbf{x} - \mathbf{x}') + \delta_{jn}\delta^3(\mathbf{x} - \mathbf{x}') = 0, \tag{20a}$$

$$D_{ji}{}^fG_{in}(\mathbf{x} - \mathbf{x}') + B_{ji}{}^f\Pi_{in}(\mathbf{x} - \mathbf{x}') - \nabla_j{}^f\phi_n(\mathbf{x} - \mathbf{x}') = 0, \tag{20b}$$

$$-\varepsilon_0\nabla^2{}^f\phi_n(\mathbf{x} - \mathbf{x}') + \nabla_i{}^f\Pi_{in}(\mathbf{x} - \mathbf{x}') = 0, \tag{20c}$$

$$C_{ji}{}^EG_{in}(\mathbf{x} - \mathbf{x}') + D_{ji}{}^E\Pi_{in}(\mathbf{x} - \mathbf{x}') = 0, \tag{20d}$$

$$D_{ji}{}^EG_{in}(\mathbf{x} - \mathbf{x}') + B_{ji}{}^E\Pi_{in}(\mathbf{x} - \mathbf{x}') - \nabla_j{}^E\phi_n(\mathbf{x} - \mathbf{x}') + \delta_{jn}\delta^3(\mathbf{x} - \mathbf{x}') = 0, \tag{20e}$$

$$-\varepsilon_0\nabla^2{}^E\phi_n(\mathbf{x} - \mathbf{x}') + \nabla_i{}^E\Pi_{in}(\mathbf{x} - \mathbf{x}') = 0. \tag{20f}$$

As evident, the first three equations [(20a)–(20c)] are the Navier-like equations for the displacement, polarization, and the potential fields corresponding to a *unit point force* (denoted by a delta function). Similarly, Eqs. (20d)–(20f) are the governing equations for the displacement, polarization, and the potential fields corresponding to a *unit point electrical field*.

Field equations (17a)–(17c) are coupled with respect to the displacement and polarization fields. The Helmholtz decomposition is frequently found to be useful to uncouple such a linked system of differential equations [wherein a vector field is expressed as the sum of the gradient of a scalar and the curl of a vector (called the solenoidal part)]. Accordingly, we decompose the displacement, polarization, body

force, and the applied electric field vectors as follows:

$$\mathbf{u} = \nabla\psi + \nabla \times \mathbf{H} \quad \nabla \cdot \mathbf{H} = 0, \tag{21a}$$

$$\mathbf{P} = \nabla\chi + \nabla \times \mathbf{K} \quad \nabla \cdot \mathbf{K} = 0, \tag{21b}$$

$$\mathbf{F} = \rho(\nabla\vartheta + \nabla \times \mathbf{L}) \quad \nabla \cdot \mathbf{L} = 0, \tag{21c}$$

$$\mathbf{E}^0 = J(\nabla\sigma + \nabla \times \mathbf{M}) \quad \nabla \cdot \mathbf{M} = 0. \tag{21d}$$

Substituting the decomposition in Eqs. (21a)–(21d) into Eqs. (17a)–(17c), and after some algebraic manipulations, the following system of uncoupled equations is obtained:

$$[-b_{11}c_{11}l'^2\nabla^2\nabla^2 + [b_{11}c_{11} - (d_{11}-f_{11})^2 + c_{11}l'^2(a+\varepsilon_0^{-1})]\nabla^2$$
$$- (a+\varepsilon_0^{-1})c_{11}]\nabla^4\psi = -\rho[b_{11}\nabla^2 - (a+\varepsilon_0^{-1})]\nabla^2\vartheta$$
$$+ Jd_{11}\nabla^4\sigma, \tag{22a}$$

$$[-b_{11}c_{11}l'^2\nabla^2\nabla^2 + [b_{11}c_{11} - (d_{11}-f_{11})^2 + c_{11}l'^2(a+\varepsilon_0^{-1})]\nabla^2$$
$$- (a+\varepsilon_0^{-1})c_{11}]\nabla^2\chi = \rho d_{11}\nabla^2\vartheta - Jc_{11}(1-l'^2\nabla^2)\nabla^2\sigma, \tag{22b}$$

$$[-(b_{44}+b_{77})c_{44}l^2\nabla^2\nabla^2 + [(b_{44}+b_{77})c_{44} - (d_{44}-f_{12})^2$$
$$+ c_{44}l^2a]\nabla^2 - ac_{44}]\nabla^4\mathbf{H} = -\rho[(b_{44}+b_{77})\nabla^2 - a]\nabla^2\mathbf{L}$$
$$+ Jd_{44}\nabla^4\mathbf{M}, \tag{22c}$$

$$[-(b_{44}+b_{77})c_{44}l^2\nabla^2\nabla^2 + [(b_{44}+b_{77})c_{44} - (d_{44}-f_{12})^2$$
$$+ c_{44}l^2a]\nabla^2 - ac_{44}]\nabla^2\mathbf{K} = \rho d_{44}\nabla^2\mathbf{L} - Jc_{44}(1$$
$$- l^2\nabla^2)\nabla^2\mathbf{M}. \tag{22d}$$

The Green's functions are derived individually for the scalar and solenoidal parts of the displacement and polarization fields and then combined appropriately to obtain the final results. Consider now a point force $\mathbf{F}$ applied parallel to the x axis; then

$$\mathbf{F} = \delta(\mathbf{r})\delta_{1i}. \tag{23}$$

The scalar part ϑ and the solenoidal part $\mathbf{L}$ of the point force $\mathbf{F}$, corresponding to Eq. (23) can be identified as

$$\vartheta = -\frac{1}{4\pi\rho}\partial_1(r^{-1}), \tag{24a}$$

$$\mathbf{L} = \frac{1}{4\pi\rho}[0, \partial_3(r^{-1}), -\partial_2(r^{-1})]. \tag{24b}$$

In order to determine the Green's function corresponding to the scalar part of the displacement ψ [see Eq. (21a)], which we denote as ${}^fG_{in}^{(1)}$, we substitute Eq. (24a) into Eq. (22a). The external electric field is set to zero since presently we are interested in the Green's functions corresponding to a point force. After carrying out the substitution, the resulting equation can be readily solved in Fourier space for $\psi(q)$ and inverted back into real space to yield ${}^fG_{in}^{(1)}$ as

$${}^fG_{ij}^{(1)}(x-x') = \frac{1}{4\pi}\partial_i\partial_j\left[\frac{A^{(1)}}{R} - \frac{B^{(1)}R}{2} + \frac{C^{(1)}}{R}e^{-R/l_1} \right.$$
$$\left. + \frac{D^{(1)}}{R}e^{-R/l_2}\right], \tag{25}$$

where $R = |\mathbf{x}-\mathbf{x}'|$.

In the above equation l_1 and l_2 are new length scale parameters which are defined implicitly via the roots of the equation below,

$$q^4 + \frac{b_{11}c_{11} - (d_{11}-f_{11})^2 + c_{11}l'^2(a+\varepsilon_0^{-1})}{b_{11}c_{11}l'^2}q^2 + \frac{(a+\varepsilon_0^{-1})}{b_{11}l'^2}$$
$$= \left(q^2 + \frac{1}{l_1^2}\right)\left(q^2 + \frac{1}{l_2^2}\right). \tag{26}$$

These roots must in general be evaluated numerically. The coefficients $A^{(1)}$, $B^{(1)}$, $C^{(1)}$ and $D^{(1)}$ can be verified to be

$$B^{(1)} = -\frac{1}{c_{11}}, \quad A^{(1)} = \frac{l'^2}{c_{11}} - \frac{(d_{11}-f_{11})^2}{c_{11}^2(a+\varepsilon_0^{-1})}$$

$$C^{(1)} = -\frac{1}{c_{11}l'^2}\frac{l_1^4l_2^2}{l_2^2-l_1^2} - \frac{(a+\varepsilon_0^{-1})}{b_{11}c_{11}l'^2}\frac{l_1^6l_2^2}{l_1^2-l_2^2}, \quad D^{(1)} =$$
$$-\frac{1}{c_{11}l'^2}\frac{l_2^4l_1^2}{l_1^2-l_2^2} - \frac{(a+\varepsilon_0^{-1})}{b_{11}c_{11}l'^2}\frac{l_2^6l_1^2}{l_2^2-l_1^2}. \tag{27}$$

By employing a procedure rather similar to the one used to obtain ${}^fG_{in}^{(1)}$, the second part of the displacement Green's function, ${}^fG_{ij}^{(2)}$, corresponding to the solenoidal part of the displacement field $\nabla \times \mathbf{H}$ can be obtained as

$${}^fG_{ij}^2 = \frac{1}{4\pi}\in_{ikl}\in_{ljm}\partial_k\partial_m\left[\frac{1}{2}E^{(1)}R + F^{(1)}I_3 + G^{(1)}I_4\right]. \tag{28}$$

In Eq. (28), the symbol I_a is defined as follows:

$$I_a = l_a^2\frac{e^{-R/l_a}-1}{R} \tag{29}$$

The following relation defines the length scales l_3 and l_4 in a manner similar to Eq. (26):

$$\left[\nabla^2\nabla^2 - \frac{(b_{44}+b_{77})c_{44} - (d_{44}-f_{12})^2 + c_{44}l^2a}{(b_{44}+b_{77})c_{44}l^2}\nabla^2 \right.$$
$$\left. + \frac{a}{(b_{44}+b_{77})l^2}\right]\nabla^4\mathbf{H} = \left(\nabla^2 - \frac{1}{l_3^2}\right)\left(\nabla^2 - \frac{1}{l_4^2}\right)\nabla^4\mathbf{H}. \tag{30}$$

The coefficients $E^{(1)}$, $F^{(1)}$, and $G^{(1)}$ in Eq. (28) are

$$E^{(1)} = \frac{1}{c_{44}}, \quad F^{(1)} = \frac{-\dfrac{1}{l_3^2} + \dfrac{a}{(b_{44}+b_{77})}}{l^2 c_{44}\left(\dfrac{1}{l_3^2}\right)\left(\dfrac{1}{l_3^2}-\dfrac{1}{l_4^2}\right)}, \quad G^{(1)}$$

$$= \frac{\dfrac{1}{l_4^2} - \dfrac{a}{(b_{44}+b_{77})}}{l^2 c_{44}\left(\dfrac{1}{l_4^2}\right)\left(\dfrac{1}{l_3^2}-\dfrac{1}{l_4^2}\right)}. \tag{31}$$

Combining the Green's functions of Eqs. (25) and (28), the net displacement Green's function $^f G_{ij}$ becomes

$$^f G_{ij} = \frac{1}{4\pi}\partial_i\partial_j\left[\frac{A^{(1)}}{R} - \frac{B^{(1)}R}{2} + \frac{C^{(1)}}{R}e^{-R/l_1} + \frac{D^{(1)}}{R}e^{-R/l_2}\right]$$
$$+ \frac{1}{4\pi}\epsilon_{ikl}\epsilon_{ljm}\partial_k\partial_m\left[\frac{1}{2}E^{(1)}R + F^{(1)}I_3 + G^{(1)}I_4\right]. \tag{32}$$

This can be further simplified to

$$^f G_{ij} = \frac{1}{4\pi}\partial_i\partial_j\left[\frac{A^{(1)}}{R} - \frac{B^{(1)}R}{2} + \frac{C^{(1)}}{R}e^{-R/l_1} + \frac{D^{(1)}}{R}e^{-R/l_2}\right]$$
$$+ \frac{1}{4\pi}\left(\delta_{ij}\nabla^2\left[\frac{1}{2}E^{(1)}R + F^{(1)}I_3 + G^{(1)}I_4\right] - \partial_i\partial_j\left[\frac{1}{2}E^{(1)}R\right.\right.$$
$$\left.\left. + F^{(1)}I_3 + G^{(1)}I_4\right]\right). \tag{33}$$

It is interesting to link our results with those of Kleinert.[40] We have seen that the inclusion of polarization-strain gradient, strain-polarization gradient, and polarization gradient-polarization gradient couplings in our internal energy expression introduced four new length scales l_1, l_2, l_3 and l_4. However, we originally had two length scales l' and l corresponding to the purely elastic strain gradient effect. So, in order to remove any contribution resulting from the polarization or its gradients from the energy expression one has to substitute $l_1 = l_2 = l'$ and $l_3 = l_4 = l$. With these substitutions, if one proceeds to evaluate the Green's function of Eq. (33), Kleinert's strain gradient Green's function for isotropic elasticity[40] is easily recovered. Since the coefficients $C^{(1)}$ and $D^{(1)}$ now correspond to the same length scale l', they can be added together. Similarly, $F^{(1)}$ and $G^{(1)}$, which correspond to l, can be added together. The following relations can be easily derived using Eqs. (26) and (30):

$$A^{(1)} = \frac{l'^2}{c_{11}}, \tag{34a}$$

$$B^{(1)} = -\frac{1}{c_{11}}, \tag{34b}$$

$$C^{(1)} + D^{(1)} = -\frac{l'^2}{c_{11}}, \tag{34c}$$

$$E^{(1)} = \frac{1}{c_{44}}, \tag{34d}$$

$$F^{(1)} + G^{(1)} = -\frac{1}{c_{44}}. \tag{34e}$$

Substituting these relations into Eq. (33), we obtain

$$^f G_{ij} = \frac{1}{4\pi\mu}\left[\frac{1}{R}(1-e^{-R/l})\right]\delta_{ij} - \frac{1}{4\pi\mu}\partial_i\partial_j\left[\frac{R}{2}+\frac{l^2}{R}(1-e^{-R/l})\right]$$
$$+ \frac{1}{4\pi(2\mu+\lambda)}\partial_i\partial_j\left[\frac{R}{2}+\frac{l'^2}{R}(1-e^{-R/l'})\right]. \tag{35}$$

Equation (35) is precisely the Green's function obtained by Kleinert[40] for strain gradient isotropic elasticity. A similar reduction on the dielectric variables allows us to make contact with the Green's function developed[30] for Mindlin's theory.

We suppress some details here as the displacement Green's function analysis given earlier may be essentially repeated to obtain from Eqs. (22b) and (22d), the Green's function $^f\Pi_{ij}$ for the induced polarization **P** due to a concentrated unit force at the origin:

$$^f\Pi_{ij} = \frac{1}{4\pi}\partial_i\partial_j\left[\frac{A^{(2)}}{R} + \frac{C^{(2)}}{R}e^{-R/l_1} + \frac{D^{(2)}}{R}e^{-R/l_2}\right]$$
$$+ \frac{1}{4\pi}\delta_{ij}\nabla^2[F^{(2)}I_3 + G^{(2)}I_4] - \frac{1}{4\pi}\partial_i\partial_j[F^{(2)}I_3 + G^{(2)}I_4]. \tag{36}$$

The coefficients $A^{(2)}$, $C^{(2)}$, $D^{(2)}$, $F^{(2)}$, and $G^{(2)}$ are given as follows:

$$A^{(2)} = \frac{d_{11}-f_{11}}{c_{11}b_{11}l'^2}l_1^2 l_2^2, \tag{37a}$$

$$C^{(2)} = \frac{d_{11}-f_{11}}{c_{11}b_{11}l'^2}\frac{l_1^4 l_2^2}{l_2^2 - l_1^2}, \tag{37b}$$

$$D^{(2)} = \frac{d_{11}-f_{11}}{c_{11}b_{11}l'^2}\frac{l_2^4 l_1^2}{l_1^2 - l_2^2}, \tag{37c}$$

$$F^{(2)} = \frac{d_{44}-f_{12}}{c_{44}(b_{44}+b_{77})}\frac{l_3^2 l_4^2}{l^2(l_4^2 - l_3^2)} = -G^{(2)}. \tag{37d}$$

From Eqs. (20c) and (36), the Green's function for the Maxwell potential $^f\phi_n$ can be written as

$$^f\phi_n = \frac{1}{4\pi\varepsilon_0}\partial_n\left[\frac{A^{(2)}}{R} + \frac{C^{(2)}}{R}e^{-R/l_1} + \frac{D^{(2)}}{R}e^{-R/l_2}\right]. \tag{38}$$

Again, the methodology to obtain the Green's functions $\{^E G_{in}, {}^E\Pi_{in}, {}^E\phi_n\}$ corresponding to a point electric field is very similar to that adopted for a point force; hence, for the sake of brevity, we simply list here the following final results:

$$4\pi \cdot {}^{f}G_{ij} = \partial_i \partial_j \left[\frac{A^{(1)}}{R} - \frac{B^{(1)}R}{2} + \frac{C^{(1)}}{R}e^{-R/l_1} + \frac{D^{(1)}}{R}e^{-R/l_2} \right]$$
$$+ \delta_{ij}\nabla^2 \left[\frac{1}{2}E^{(1)}R + F^{(1)}I_3 + G^{(1)}I_4 \right] - \partial_i \partial_j \left[\frac{1}{2}E^{(1)}R \right.$$
$$\left. + F^{(1)}I_3 + G^{(1)}I_4 \right], \tag{39a}$$

$$4\pi \cdot {}^{f}\Pi_{ij} = 4\pi \cdot {}^{E}G_{ij} = \partial_i \partial_j \left[\frac{A^{(2)}}{R} + \frac{C^{(2)}}{R}e^{-R/l_1} + \frac{D^{(2)}}{R}e^{-R/l_2} \right]$$
$$+ \delta_{ij}\nabla^2[F^{(2)}I_3 + G^{(2)}I_4] - \partial_i \partial_j[F^{(2)}I_3 + G^{(2)}I_4], \tag{39b}$$

$$4\pi\varepsilon_0 \cdot {}^{f}\phi_n = \partial_n \left[\frac{A^{(2)}}{R} + \frac{C^{(2)}}{R}e^{-R/l_1} + \frac{D^{(2)}}{R}e^{-R/l_2} \right], \tag{39c}$$

$$4\pi \cdot {}^{E}\Pi_{ij} = \partial_i \partial_j \left[\frac{A^{(3)}}{R} + \frac{C^{(3)}}{R}e^{-R/l_1} + \frac{D^{(3)}}{R}e^{-R/l_2} \right] + \delta_{ij}\nabla^2[F^{(3)}I_3$$
$$+ G^{(3)}I_4] - \partial_i \partial_j[F^{(3)}I_3 + G^{(3)}I_4], \tag{39d}$$

$$4\pi\varepsilon_0 \cdot {}^{E}\phi_n = \partial_n \left[\frac{A^{(3)}}{R} + \frac{C^{(3)}}{R}e^{-R/l_1} + \frac{D^{(3)}}{R}e^{-R/l_2} \right]. \tag{39e}$$

The coefficients $A^{(3)}$, $C^{(3)}$, $D^{(3)}$, $F^{(3)}$, and $G^{(3)}$ introduced in the Eqs. (39d) and (39e) are

$$A^{(3)} = -\frac{l_1^2 l_2^2}{b_{11}l'^2}, \tag{40a}$$

$$C^{(3)} = -\frac{1}{b_{11}l'^2}\frac{l_1^4 l_2^2}{l_2^2 - l_1^2} + \frac{l_2^2 l_1^2}{b_{11}(l_2^2 - l_1^2)}, \tag{40b}$$

$$D^{(3)} = -\frac{1}{b_{11}l'^2}\frac{l_2^4 l_1^2}{l_1^2 - l_2^2} + \frac{l_2^2 l_1^2}{b_{11}(l_1^2 - l_2^2)}, \tag{40c}$$

$$F^{(3)} = \frac{1}{(b_{44} + b_{77})}\frac{(1/l^2) - (1/l_3^2)}{(1/l_3^2) - (1/l_4^2)} = -G^{(3)}. \tag{40d}$$

${}^{f}\Pi_{ij}$ is equal to ${}^{E}G_{ij}$, which is no surprise. By employing an analogue of the classical Betti's reciprocal theorem for elastic dielectrics, this equality can be rigorously proved.[43]

Further, we note that the positive definiteness requirement of the energy density functional[9] forces the material length scale constants l_1, l_2, l_3, and l_4 introduced in our theory to obey the following constraining relations:

$$l_1^2 + l_2^2 > l'^2, \quad l_3^2 + l_4^2 > l^2. \tag{41}$$

IV. THE GENERAL EMBEDDED INCLUSION PROBLEM

Consider an arbitrary shaped inclusion with a prescribed stress-free transformation strain $\boldsymbol{\varepsilon}^*$ in its domain (Ω), located in an infinite isotropic medium (D). In various physical prob-

lems, the transformation strain can represent thermal mismatch, lattice mismatch, phase transformation, and other inelastic transformations. Following Eshelby's[33] well-known formalism, the constitutive laws of Eqs. (16a)–(16d) assume the following form in the absence of external body force and electric field:

$$t_{ij} = [c_{12}\delta_{ij}\delta_{ps} + 2c_{44}\delta_{ip}\delta_{js}](\varepsilon_{ps} - \varepsilon_{ps}^*) + [d_{12}\delta_{ij}\delta_{ps} + d_{44}(\delta_{is}\delta_{jp} + \delta_{js}\delta_{ip})]P_{p,s}, \tag{42a}$$

$$t_{ijm,m} = [(c_{12} + 2c_{44})l'^2\nabla^2\delta_{ij}\delta_{ps} + c_{44}l^2\nabla^2(\delta_{is}\delta_{jp} - \delta_{js}\delta_{ip})](u_{p,s} - \varepsilon_{ps}^*) + [f_{12}\delta_{pi}\delta_{js} + f_{44}(\delta_{ps}\delta_{ji} + \delta_{is}\delta_{jp})]P_{p,s}, \tag{42b}$$

$$E_{ij} = [d_{12}\delta_{ij}\delta_{ps} + d_{44}(\delta_{is}\delta_{jp} + \delta_{js}\delta_{ip})](u_{p,s} - \varepsilon_{ps}^*) + [b_{12}\delta_{ij}\delta_{ps} + (b_{44} + b_{77})\delta_{is}\delta_{jp} + (b_{44} - b_{77})\delta_{js}\delta_{ip}]P_{p,s}, \tag{42c}$$

$$E_i = -\{aP_i + [f_{12}\delta_{ij}\delta_{ps} + f_{44}(\delta_{is}\delta_{jp} + \delta_{js}\delta_{ip})](u_{j,ps} - \varepsilon_{jp,s}^*)\}. \tag{42d}$$

In Eqs. (42a)–(42d), $\boldsymbol{\varepsilon}$ is the total strain compatible with Eq. (4). Substituting, Eqs. (42a)–(42d) in the balance laws for the problem given by Eqs. (11), we obtain

$$C_{ij}u_j + D_{ij}P_j = [c_{12}\delta_{ij}\delta_{ps} + 2c_{44}\delta_{ip}\delta_{js}]\varepsilon_{ps,j}^* - [(c_{12} + 2c_{44})l'^2\nabla^2\delta_{ij}\delta_{ps} + c_{44}l^2\nabla^2(\delta_{is}\delta_{jp} - \delta_{js}\delta_{ip})]\varepsilon_{ps,j}^*, \tag{43a}$$

$$D_{ij}u_j + B_{ij}P_j - \phi_{,i} = [(d_{12} - f_{44})\delta_{ij}\delta_{ps} + (d_{44} - f_{44})\delta_{is}\delta_{jp} + (d_{44} - f_{12})\delta_{js}\delta_{ip}]\varepsilon_{ps,j}^*. \tag{43b}$$

Comparing Eqs. (43) with Eqs. (18), we can immediately see that the terms on its right-hand side of Eqs. (43a) and (43b) act like a fictitious body force and electric field respectively. The displacement field $u_i(\mathbf{x})$ due to this body force and electric field can be easily written with the help of the Green's functions that we derived in Sec. III.

$$u_i(\mathbf{x}) = -\int {}^{f}G_{ij}(\mathbf{x} - \mathbf{x}')[c_{12}\delta_{jl}\delta_{mn} + 2c_{44}\delta_{jm}\delta_{ln} - (c_{12} + 2c_{44})l'^2\nabla^2\delta_{lj}\delta_{mn} - c_{44}l^2\nabla^2(\delta_{jn}\delta_{lm} - \delta_{ln}\delta_{jm})]\varepsilon_{mn,l}^*(\mathbf{x}')d\mathbf{x}' - \int {}^{E}G_{ij}(\mathbf{x} - \mathbf{x}')[(d_{12} - f_{44})\delta_{jl}\delta_{mn} + (2d_{44} - f_{12} - f_{44})\delta_{jm}\delta_{ln}]\varepsilon_{mn,l}^*(\mathbf{x}')d\mathbf{x}'. \tag{44}$$

The polarization field $P_i(\mathbf{x})$ follows in a similar manner.

$$P_i(\mathbf{x}) = -\int {}^{f}\Pi_{ij}(\mathbf{x} - \mathbf{x}')[c_{12}\delta_{jl}\delta_{mn} + 2c_{44}\delta_{jm}\delta_{ln} - (c_{12} + 2c_{44})l'^2\nabla^2\delta_{lj}\delta_{mn} - c_{44}l^2\nabla^2(\delta_{jn}\delta_{lm} - \delta_{ln}\delta_{jm})]\varepsilon_{mn,l}^*(\mathbf{x}')d\mathbf{x}' - \int {}^{E}\Pi_{ij}(\mathbf{x} - \mathbf{x}')[(d_{12}$$

$$-f_{44})\delta_{jl}\delta_{mn}+(2d_{44}-f_{12}-f_{44})\delta_{jm}\delta_{ln}]\varepsilon^*_{mn,l}(\mathbf{x}')\mathrm{d}\mathbf{x}'. \tag{45}$$

Integrating Eqs. (44) and (45) by parts and assuming that the boundary terms vanish, we have

$$u_i(\mathbf{x})=-\int\,[c_{12}\delta_{jl}\delta_{mn}+2c_{44}\delta_{jm}\delta_{ln}-(c_{12}+2c_{44})l'^2\nabla^2\delta_{lj}\delta_{mn}$$
$$-c_{44}l^2\nabla^2(\delta_{jn}\delta_{lm}-\delta_{ln}\delta_{jm})]\varepsilon^*_{mn}(\mathbf{x}')^f G_{ij,l}(\mathbf{x}-\mathbf{x}')\mathrm{d}\mathbf{x}'$$
$$-\int\,[(d_{12}-f_{44})\delta_{jl}\delta_{mn}+(2d_{44}-f_{12}$$
$$-f_{44})\delta_{jm}\delta_{ln}]\varepsilon^*_{mn}(\mathbf{x}')^E G_{ij,l}(\mathbf{x}-\mathbf{x}')\mathrm{d}\mathbf{x}', \tag{46a}$$

$$P_i(\mathbf{x})=-\int\,[c_{12}\delta_{jl}\delta_{mn}+2c_{44}\delta_{jm}\delta_{ln}-(c_{12}+2c_{44})l'^2\nabla^2\delta_{lj}\delta_{mn}$$
$$-c_{44}l^2\nabla^2(\delta_{jn}\delta_{lm}-\delta_{ln}\delta_{jm})]\varepsilon^*_{mn}(\mathbf{x}')^f \Pi_{ij,l}(\mathbf{x}-\mathbf{x}')\mathrm{d}\mathbf{x}'$$
$$-\int\,[(d_{12}-f_{44})\delta_{jl}\delta_{mn}+(2d_{44}-f_{12}$$
$$-f_{44})\delta_{jm}\delta_{ln}]\varepsilon^*_{mn}(\mathbf{x}')^E \Pi_{ij,l}(\mathbf{x}-\mathbf{x}')\mathrm{d}\mathbf{x}'. \tag{46b}$$

In the spirit of Eshelby's formalism, given a uniform transformation strain, the displacement field $u_i(\mathbf{x})$ and the polarization field $P_i(\mathbf{x})$, can be cast in terms of certain potentials $\phi(\mathbf{x})$, $\psi(\mathbf{x})$ and $M^a(\mathbf{x})$:

$$u_i(\mathbf{x})=-[c_{12}\varepsilon^*_{mm}\delta_{jl}+2c_{44}\varepsilon^*_{jl}]\cdot\left[\left(A^{(1)}\phi_{,ijl}-\frac{B^{(1)}}{2}\psi_{,ijl}\right.\right.$$
$$+C^{(1)}M^1_{,ijl}+D^{(1)}M^2_{,ijl}\bigg)+\delta_{ij}(E^{(1)}\phi_{,l}+F^{(1)}M^3_{,l}$$
$$+G^{(1)}M^4_{,l})-\left(\frac{E^{(1)}}{2}\psi_{,ijl}-(F^{(1)}l^2_3+G^{(1)}l^2_4)\phi_{,ijl}\right.$$
$$+F^{(1)}l^2_3 M^3_{,ijl}+G^{(1)}l^2_4 M^4_{,ijl}\bigg)\bigg]-[(d_{12}-f_{44})\varepsilon^*_{mm}\delta_{jl}$$
$$+(2d_{44}-f_{12}-f_{44})\varepsilon^*_{jl}]\cdot[(A^{(2)}\phi_{,ijl}+C^{(2)}M^1_{,ijl}$$
$$+D^{(2)}M^2_{,ijl})+\delta_{ij}(F^{(2)}M^3_{,l}+G^{(2)}M^4_{,l})-[F^{(2)}l^2_3 M^3_{,ijl}$$
$$+G^{(2)}l^2_4 M^4_{,ijl}-(F^{(2)}l^2_3+G^{(2)}l^2_4)\phi_{,ijl}]]. \tag{47}$$

$$P_i(\mathbf{x})=-[c_{12}\varepsilon^*_{mm}\delta_{jl}+2c_{44}\varepsilon^*_{jl}]\cdot[(A^{(2)}\phi_{,ijl}+C^{(2)}M^1_{,ijl}$$
$$+D^{(2)}M^2_{,ijl})+\delta_{ij}(F^{(2)}M^3_{,l}+G^{(2)}M^4_{,l})-(F^{(2)}l^2_3 M^3_{,ijl}$$
$$+G^{(2)}l^2_4 M^4_{,ijl})+(F^{(2)}l^2_3+G^{(2)}l^2_4)\phi_{,ijl}]-[(d_{12}$$
$$-f_{44})\varepsilon^*_{mm}\delta_{jl}+(2d_{44}-f_{12}-f_{44})\varepsilon^*_{jl}]\cdot[(A^{(3)}\phi_{,ijl}$$
$$+C^{(3)}M^1_{,ijl}+D^{(3)}M^2_{,ijl})+\delta_{ij}(F^{(3)}M^3_{,l}+G^{(3)}M^4_{,l})$$
$$-F^{(3)}l^2_3 M^3_{,ijl}+G^{(3)}l^2_4 M^4_{,ijl}+(F^{(3)}l^2_3+G^{(3)}l^2_4)\phi_{,ijl}]. \tag{48}$$

The potentials $\varphi(\mathbf{x})$ and $\psi(\mathbf{x})$ are the harmonic and biharmonic potentials while $M^a(\mathbf{x})$ is the so-called Yukawa potential. These potentials are defined below as

$$\phi(\mathbf{x})=\frac{1}{4\pi}\int_\Omega\frac{1}{R}\mathrm{d}\mathbf{x}', \tag{49a}$$

$$\psi(\mathbf{x})=\frac{1}{4\pi}\int_\Omega R\,\mathrm{d}\mathbf{x}', \tag{49b}$$

$$M^a(\mathbf{x})=\frac{1}{4\pi}\int_\Omega\frac{e^{-R/l_a}}{R}\mathrm{d}\mathbf{x}'. \tag{49c}$$

R is $|\mathbf{x}-\mathbf{x}'|$. The classical part of the displacement field of Eq. (46a) and (46b) can be identified as

$$-(c_{12}\varepsilon^*_{mm}\delta_{jl}+2c_{44}\varepsilon^*_{jl})\left[-\frac{B^{(1)}}{2}\psi_{,ijl}+\delta_{ij}E^{(1)}\phi_{,l}-\frac{E^{(1)}}{2}\psi_{,ijl}\right]. \tag{50}$$

On the other hand, the expression for the polarization Eq. (47) has no classical counterpart since the material is isotropic and hence nonpiezoelectric.

The total strain $\boldsymbol{\varepsilon}$ can then be written from Eq. (47) and Eq. (4) as

$$\varepsilon_{ik}(\mathbf{x})=-[c_{12}\varepsilon^*_{mm}\delta_{jl}+2c_{44}\varepsilon^*_{jl}]\cdot\left[\left(A^{(1)}\phi_{,ijlk}-\frac{B^{(1)}}{2}\psi_{,ijlk}\right.\right.$$
$$+C^{(1)}M^1_{,ijlk}+D^{(1)}M^2_{,ijlk}\bigg)$$
$$+\frac{\delta_{ij}(E^{(1)}\phi_{,lk}+F^{(1)}M^3_{,lk}+G^{(1)}M^4_{,lk})}{2}$$
$$+\frac{\delta_{kj}(E^{(1)}\phi_{,li}+F^{(1)}M^3_{,li}+G^{(1)}M^4_{,li})}{2}-\left(\frac{E^{(1)}}{2}\psi_{,ijlk}\right.$$
$$+F^{(1)}l^2_3 M^3_{,ijlk}+G^{(1)}l^2_4 M^4_{,ijlk}-(F^{(1)}l^2_3+G^{(1)}l^2_4)\phi_{,ijlk}\bigg)\bigg]$$
$$-[(d_{12}-f_{44})\varepsilon^*_{mm}\delta_{jl}+(2d_{44}-f_{12}$$
$$-f_{44})\varepsilon^*_{jl}]\cdot\left[(A^{(2)}\phi_{,ijlk}+C^{(2)}M^1_{,ijlk}+D^{(2)}M^2_{,ijlk})\right.$$
$$+\frac{\delta_{ij}(F^{(2)}M^3_{,lk}+G^{(2)}M^4_{,lk})}{2}+\frac{\delta_{kj}(F^{(2)}M^3_{,li}+G^{(2)}M^4_{,li})}{2}$$
$$-(F^{(2)}l^2_3 M^3_{,ijlk}+G^{(2)}l^2_4 M^4_{,ijlk}-(F^{(2)}l^2_3+G^{(2)}l^2_4)\phi_{,ijlk})\bigg]. \tag{51}$$

The trace of the strain (dilatation), which is of frequent physical interest, can be expressed as

$$tr(\varepsilon_{jl})=-[c_{12}\varepsilon^*_{mm}\delta_{jl}+2c_{44}\varepsilon^*_{jl}]\cdot\left[\left(A^{(1)}\phi_{,jlmm}-\frac{B^{(1)}}{2}\psi_{,jlmm}\right.\right.$$
$$+C^{(1)}M^1_{,jlmm}+D^{(1)}M^2_{,jlmm}\bigg)+(E^{(1)}\phi_{,jl}+F^{(1)}M^3_{,jl}$$
$$+G^{(1)}M^4_{,jl})-\left(\frac{E^{(1)}}{2}\psi_{,jlmm}+F^{(1)}l^2_3 M^3_{,jlmm}\right.$$

$$+ G^{(1)}l_4^2 M^4_{,jlmm} - (F^{(1)}l_3^2 + G^{(1)}l_4^2)\phi_{,jlmm}\Bigg)\Bigg] - [(d_{12}$$

$$- f_{44})\varepsilon^*_{mm}\delta_{jl} + (2d_{44} - f_{12} - f_{44})\varepsilon^*_{jl}] \cdot [(A^{(2)}\phi_{,jlmm}$$

$$+ C^{(2)}M^1_{,jlmm} + D^{(2)}M^2_{,jlmm}) + (F^{(2)}M^3_{,jl} + G^{(2)}M^4_{,jl})$$

$$- (F^{(2)}l_3^2 M^3_{,jlmm} + G^{(2)}l_4^2 M^4_{,jlmm} - (F^{(2)}l_3^2$$

$$+ G^{(2)}l_4^2)\phi_{,jlmm})]. \tag{52}$$

V. EXPLICIT RESULTS FOR SPHERICAL AND CYLINDRICAL INCLUSIONS

Our results in the preceding section are quite general but lead to rather cumbersome expressions (albeit closed form) even for the highly symmetrical spherical and cylindrical shapes. In the present section, we restrict our presentation to dilatational transformation strains as (relatively speaking) simple and elegant expressions can be derived for this case. We hasten to point out though that the derived expressions in the preceding and present section can be used, with only minor algebra, to deduce the results for other types of transformation strains such as shear. We do not present those for the sake of brevity. Indeed, for several problems of technological interest (i.e., lattice mismatched quantum dots, thermal inclusions), the mismatch is dilatational in nature.

Consider a spherical inclusion of radius a with a domain Ω embedded in an infinite matrix containing a constant dilatational transformation strain. Our results in the previous section for the strain and the polarization fields were cast in terms of three potentials, the harmonic potential $\varphi(\mathbf{x})$, the biharmonic potential $\psi(\mathbf{x})$, and the Yukawa potential $M^a(\mathbf{x})$. For the spherical shape, closed form expressions exist for these potentials.[44–46]

The potentials due to the spherical inclusion for points inside it, i.e., $R \in \Omega$, are

$$\psi(R) = -\frac{1}{60}(R^4 - 10a^2R^2 - 5a^4), \tag{53a}$$

$$\varphi(R) = -\frac{1}{6}(R^2 - 3a^2), \tag{53b}$$

$$M^a(R) = l_a^2 - l_a^2(l_a + a)e^{a/l_a}\frac{sh(R/l_a)}{R}. \tag{53c}$$

For points outside the inclusion, i.e., $R \notin \Omega$, the potentials become

$$\psi(R) = \frac{a^3}{15}\left(5R + \frac{a^2}{R}\right), \tag{54a}$$

$$\varphi(R) = \frac{a^3}{3R}, \tag{54b}$$

$$M^a(R) = l_a^2[a \cdot ch(a/l_a) - l_a \cdot sh(a/l_a)]\frac{e^{-R/l_a}}{R}. \tag{54c}$$

A constant dilatational transformation strain can be expressed as

$$\varepsilon^*_{ij} = \varepsilon^*\delta_{ij} \tag{55}$$

Substituting Eq. (55) in Eq. (52), and with the aid of the potentials defined in Eqs. (53a)–(53c), we arrive at the following expression for the trace of strain at a point inside the inclusion ($R \in \Omega$):

$$tr(\varepsilon_{jl}) = (3c_{12} + 2c_{44})\varepsilon^* \cdot \left(-B^{(1)} + C^{(1)}\frac{l_1 + a}{l_1^2}e^{-a/l_1}\frac{sh(R/l_1)}{R}\right.$$

$$\left. + D^{(1)}\frac{l_2 + a}{l_2^2}e^{-a/l_2}\frac{sh(R/l_2)}{R}\right) + [3(d_{12} - f_{12}) + 2(d_{44}$$

$$- f_{44})]\varepsilon^* \cdot \left(C^{(2)}\frac{l_1 + a}{l_1^2}e^{-a/l_1}\frac{sh(R/l_1)}{R}\right.$$

$$\left. + D^{(2)}\frac{l_2 + a}{l_2^2}e^{-a/l_2}\frac{sh(R/l_2)}{R}\right). \tag{56}$$

The trace of the strain for points outside the inclusion ($R \notin \Omega$) can also be obtained from Eqs. (52) and (54a)–(54c),

$$tr(\varepsilon_{jl}) = (3c_{12} + 2c_{44})\varepsilon^* \cdot \left(C^{(1)}\frac{a \cdot ch(a/l_1) - l_1 \cdot sh(a/l_1)}{l_1^2}\frac{e^{-R/l_1}}{R}\right.$$

$$\left. + D^{(1)}\frac{a \cdot ch(a/l_2) - l_2 \cdot sh(a/l_2)}{l_2^2}\frac{e^{-R/l_2}}{R}\right) + [3(d_{12} - f_{12})$$

$$+ 2(d_{44}$$

$$- f_{44})]\varepsilon^* \cdot \left(C^{(2)}\frac{a \cdot ch(a/l_1) - l_1 \cdot sh(a/l_1)}{l_1^2}\frac{e^{-R/l_1}}{R}\right.$$

$$\left. + D^{(2)}\frac{a \cdot ch(a/l_2) - l_2 \cdot sh(a/l_2)}{l_2^2}\frac{e^{-R/l_2}}{R}\right). \tag{57}$$

If we neglect both the flexoelectric and purely nonlocal elastic gradient effects, then the dilatation reduces to the well-known result in classical elasticity,[33]

$$tr(\varepsilon_{jl}) = \begin{cases} \dfrac{3c_{12} + 2c_{44}}{c_{12} + 2c_{44}}\varepsilon^* & R \in \Omega \\ 0 & R \notin \Omega \end{cases} \tag{58}$$

The dilatational strain results from Eqs. (56) and (57) have been plotted after suitable normalization for various inclusion sizes as a function of position in Fig. 3. The location $R = a$ indicates the boundary of the spherical inclusion. We note that our results are clearly size dependent. Unlike the classical solution, which predicts that the dilatation is constant inside the inclusion and zero outside, our solution is inhomogeneous within the inclusion and converges asymptotically to classical elasticity for large inclusion sizes.

Another point worth mentioning is that the dilatation of strain solely depends upon the strain gradient length scale l' and associated length scales of l_1 and l_2. There is no dependence on l or the associated length scales of l_3 and l_4. This is due to the fact that the length scale parameter l (and thereby l_3 and l_4) is physically associated with couple stresses or gradients of the rotation vector. For inclusion sizes beyond
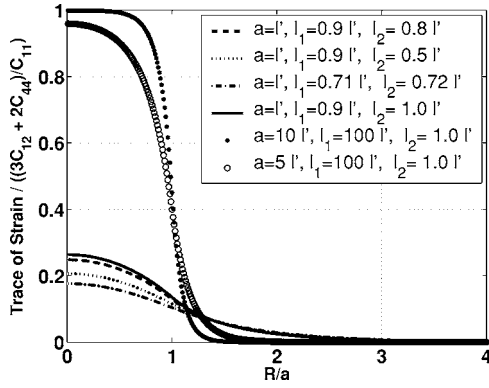
FIG. 3. Normalized strain dilatation as a function of position (R) and inclusion size (a) for a spherical inclusion.

ten times the purely elastic characteristic length scale, the flexoelectric solution is fairly close to the classical one except at points very close to the interface. We note in passing that, as expected, the sharp interface of the inclusion-matrix becomes "diffuse."

To explicitly display the size dependency of our solution, we also plot (Fig. 4) the dilatation as a function of size for two fixed positions. Evidently (and hardly surprisingly), the flexoelectric and nonlocal effects are more predominant close to the interface and are much smaller at the center of the inclusion.

From Eq. (48), the polarization P_i for an inclusion can be written as

$$P_i(\mathbf{x}) = -(3c_{12} + 2c_{44})\varepsilon^* \cdot \partial_i(A^{(2)}\phi_{,kk} + C^{(2)}M^1_{,kk} + D^{(2)}M^2_{,kk})$$
$$- [3(d_{12} - f_{12}) + 2(d_{44} - f_{44})]\varepsilon^* \cdot \partial_i(A^{(3)}\phi_{,kk}$$
$$+ C^{(3)}M^1_{,kk} + D^{(3)}M^2_{,kk}). \tag{59}$$

Substituting the potentials from Eqs. (53a)–(53c), the polarization for interior points ($|\mathbf{x}| = R \in \Omega$) becomes
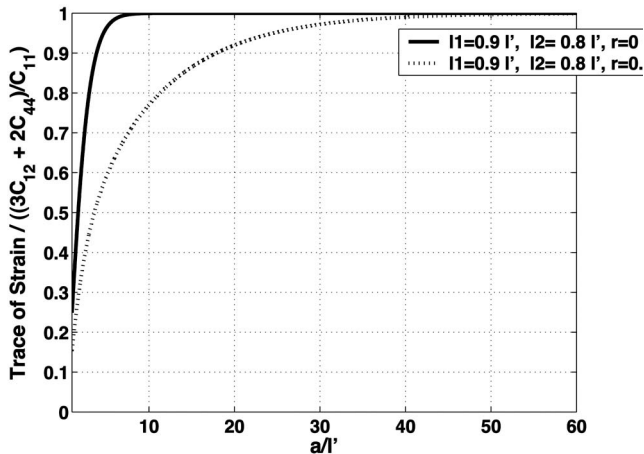

FIG. 4. Dilatational strain as a function of size (a) for fixed position (r) inside a spherical inclusion.

$$P_i(\mathbf{x}) = (3c_{12} + 2c_{44})\varepsilon^* \cdot \partial_i\left[C^{(2)}\frac{e^{-a/l_1}(a + l_1)\,.\,sh(R/l_1)}{R} \right.$$
$$+ D^{(2)}\frac{e^{-a/l_2}(a + l_2)\cdot sh(R/l_2)}{R}\right] + [3(d_{12} - f_{12}) + 2(d_{44}$$
$$- f_{44})]\varepsilon^* \cdot \partial_i\left[C^{(3)}\frac{e^{-a/l_1}(a + l_1)\cdot sh(R/l_1)}{R} \right.$$
$$+ D^{(3)}\frac{e^{-a/l_2}(a + l_2)\cdot sh(R/l_2)}{R}\right]. \tag{60}$$

For exterior points ($R \notin \Omega$), from Eqs. (54a)–(54c), the polarization is

$$P_i(\mathbf{x}) = -(3c_{12} + 2c_{44})\varepsilon^* \cdot \partial_i\left[C^{(2)}\frac{e^{-R/l_1}}{R}\Gamma^1_a + D^{(2)}\frac{e^{-R/l_2}}{R}\Gamma^2_a\right]$$
$$+ [3(d_{12} - f_{12}) + 2(d_{44} - f_{44})]\varepsilon^* \cdot \partial_i\left[C^{(3)}\frac{e^{-R/l_1}}{R}\Gamma^1_a\right.$$
$$+ D^{(3)}\frac{e^{-R/l_2}}{R}\Gamma^2_a\right], \tag{61a}$$

$$\Gamma^i_a = a \cdot ch(a/l_i) - l_i \cdot sh(a/l_i). \tag{61b}$$

The magnitude of the polarization field $P(\mathbf{x})$ for interior points may be written ($R \in \Omega$) as:

$$P(\mathbf{x}) = (3c_{12} + 2c_{44})\varepsilon^* \cdot \left(C^{(2)}\frac{e^{-a/l_1}(a + l_1)\Gamma^1_R}{R^2 l_1}\right.$$
$$+ D^{(2)}\frac{e^{-a/l_2}(a + l_2)\Gamma^2_R}{R^2 l_2}\right) + [3(d_{12} - f_{12}) + 2(d_{44}$$
$$- f_{44})]\varepsilon^* \cdot \left(C^{(3)}\frac{e^{-a/l_1}(a + l_1)\Gamma^1_R}{R^2 l_1}\right.$$
$$+ D^{(3)}\frac{e^{-a/l_2}(a + l_2)\Gamma^2_R}{R^2 l_2}\right). \tag{62}$$

Likewise, for exterior points ($R \notin \Omega$), the magnitude is:

$$P(\mathbf{x}) = (3c_{12} + 2c_{44})\varepsilon^* \cdot \left(C^{(2)}\frac{e^{-R/l_1}(R + l_1)\Gamma^1_a}{R^2 l_1}\right.$$
$$+ D^{(2)}\frac{e^{-R/l_2}(R + l_2)\Gamma^2_a}{R^2 l_2}\right) + [3(d_{12} - f_{12}) + 2(d_{44}$$
$$- f_{44})]\varepsilon^* \cdot \left(C^{(3)}\frac{e^{-a/l_1}(a + l_1)\Gamma^1_a}{R^2 l_1}\right.$$
$$+ D^{(3)}\frac{e^{-a/l_2}(a + l_2)\Gamma^2_a}{R^2 l_2}\right). \tag{63}$$

Figure 5 shows the variation of the magnitude of polarization with position for various inclusion sizes.

Figure 5 is a dramatic result. The materials are nonpiezoelectric and yet, due to the presence of strain gradients, there exists a finite polarization in and around the inclusion. At positions far away from the inclusion, the polarization
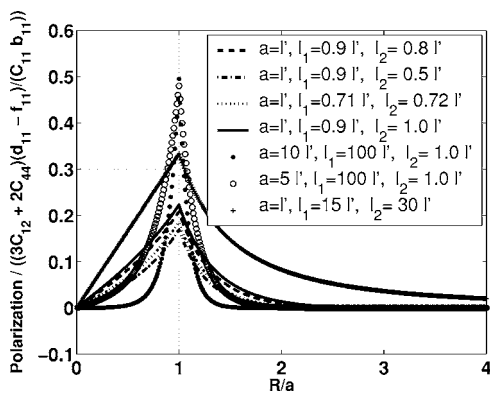
FIG. 5. Magnitude of polarization as a function of position (R) and inclusion size (a) for a spherical inclusion.

asymptotically tends to zero as it should. There are some subtle effects that need to be discussed with regards to the electric fields in inclusions due to the flexoelectric effect. For a more visually appealing interpretation, the reader is referred to Fig. 6 where we contour plot the electric fields at different positions as a function of size and material property combinations (i.e., different combination of the characteristic lengths). Darker regions indicate low polarization while lighter shade indicates a higher concentration.

One may intuitively expect that electric fields disappear for "large" inclusions sizes. This is correct, as borne out by both Figs. 5 and 6, except at the interface where electric fields persist regardless of size. However, as the size increases, the electric field becomes increasingly localized in thinner and thinner layers at the interface. Interestingly, the electric fields for a given location reach a maximum for

some size that depends on the characteristic length scales. The plots in the second row of Fig. 6 are for a constant size and show a rich interplay between the characteristic length scales. This is consistent with the one-dimensional solutions[6] for simple layered structures (in the context of Mindlin's restricted reverse flexoelectric theory). It should, however, be pointed out that no physical meaning may be attached to the magnitudes of the electric fields for the plots in the second row of Fig. 6 since we are comparing normalized values for *different* materials (characterized by different values of the length scale parameters). To be more concrete, we choose InAs-GaAs as an example inclusion-matrix system. Both are important quantum dot materials and subject to a large lattice mismatch-induced dilatational transformation mismatch strain ∼6.7%. For our estimates, we ignore the elastic modulus difference between these two materials.[47] Some of the material properties used for our estimates (including the calculated characteristic length scales) are listed in Ref. 48. We then find that for an inclusion size of 10 μm, the electric field at the interface is ∼750 kV/m which, qualitatively consistent with Figs. 5 and 6, drops to ∼1.33% closer to the center ($a/10$). The electric fields penetrate well beyond the interface for smaller sizes and for a size of 5 nm, the drop to a radial location of $a/10$ is nearly 11% of the value at the interface and numerically nearly thrice as that for 10 μm at the same location.

Consider now an infinitely long cylindrical inclusion occupying radius a with domain Ω embedded inside an infinite isotropic medium with a constant dilatational transformation strain, ε^*. For a cylindrical inclusion the Yukawa potential $M^{(a)}$ is given as[43]
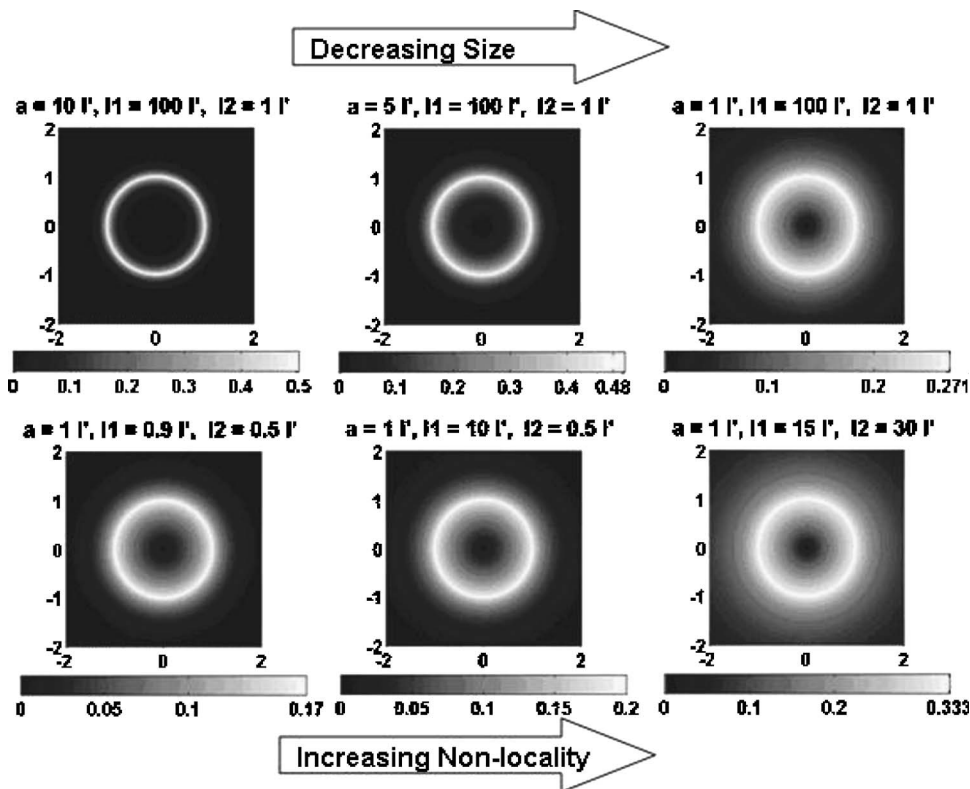

FIG. 6. Normalized contour plots of the electric fields around the spherical inclusion for different sizes and characteristic length scales.

$$M^a(R) = \left\{ l_a R \cdot \left[I_1\left(\frac{R}{l_a}\right) K_0\left(\frac{R}{l_a}\right) + K_1\left(\frac{R}{l_a}\right) I_0\left(\frac{R}{l_a}\right) \right] \right.$$

$$\left. - l_a a \cdot K_1\left(\frac{a}{l_a}\right) I_0\left(\frac{R}{l_a}\right) \right\} \quad R \in \Omega \quad , \quad (64a)$$

$$M^a(R) = \left\{ l_a a \cdot I_1\left(\frac{R}{l_a}\right) K_0\left(\frac{R}{l_a}\right) \right\} \quad R \notin \Omega \quad . \quad (64b)$$

Substituting the potentials from Eq. (64a) into Eq. (52), the dilatation of strain at a point inside the cylindrical inclusion ($R \in \Omega$) can be expressed as

$$tr(\varepsilon_{jl}) = (3c_{12} + 2c_{44})\varepsilon^* \cdot \left[\frac{1}{c_{11}} + C^{(1)}\left(\frac{a \cdot I_0(R/l_1)K_1(a/l_1)}{l_1^3} \right) \right.$$

$$+ D^{(1)}\left(\frac{a \cdot I_0(R/l_2)K_1(a/l_2)}{l_2^3} \right) \right] + \left[3(d_{12} - f_{12}) + 2(d_{44} \right.$$

$$- f_{44})]\varepsilon^* \cdot \left[C^{(2)}\left(\frac{a \cdot I_0(R/l_1)K_1(a/l_1)}{l_1^3} \right) + D^{(2)} \right.$$

$$\times \left(\frac{a \cdot I_0(R/l_2)K_1(a/l_2)}{l_2^3} \right) \right]. \quad (65)$$

For a point outside the inclusion ($R \notin \Omega$), the trace of strain is

$$tr(\varepsilon_{jl}) = (3c_{12} + 2c_{44})\varepsilon^* \cdot \left[C^{(1)}\left(\frac{a \cdot I_1(a/l_1)K_0(R/l_1)}{l_1^3} \right) + D^{(1)} \right.$$

$$\times \left(\frac{a \cdot I_1(a/l_2)K_0(R/l_2)}{l_2^3} \right) \right] + \left[3(d_{12} - f_{12}) + 2(d_{44} \right.$$

$$- f_{44})]\varepsilon^* \cdot \left[C^{(2)}\left(\frac{a \cdot I_1(a/l_1)K_0(R/l_1)}{l_1^3} \right) + D^{(2)} \right.$$

$$\times \left(\frac{a \cdot I_1(a/l_2)K_0(R/l_2)}{l_2^3} \right) \right]. \quad (66)$$

The polarization P_i for a point inside the inclusion ($R \in \Omega$) can also be as

$$P_i(\mathbf{x}) = (3c_{12} + 2c_{44})\varepsilon^* \cdot \partial_i \left[C^{(2)}\frac{a \cdot I_0(R/l_1)K_1(a/l_1)}{l_1} \right.$$

$$+ D^{(2)}\frac{a \cdot I_0(R/l_2)K_1(a/l_2)}{l_2} \right] + \left[3(d_{12} - f_{12}) + 2(d_{44} \right.$$

$$- f_{44})]\varepsilon^* \cdot \partial_i \left[C^{(3)}\frac{a \cdot I_0(R/l_1)K_1(a/l_1)}{l_1} \right.$$

$$+ D^{(3)}\frac{a \cdot I_0(R/l_2)K_1(a/l_2)}{l_2} \right]. \quad (67)$$

For a point outside the inclusion ($R \notin \Omega$), the polarization becomes:

$$P_i(\mathbf{x}) = (3c_{12} + 2c_{44})\varepsilon^* \cdot \partial_i \left[C^{(2)}\frac{a \cdot I_1(a/l_1)K_1(R/l_1)}{l_1} \right.$$

$$+ D^{(2)}\frac{a \cdot I_1(a/l_2)K_0(R/l_2)}{l_2} \right] + \left[3(d_{12} - f_{12}) + 2(d_{44} \right.$$

$$- f_{44})]\varepsilon^* \cdot \partial_i \left[C^{(3)}\frac{a \cdot I_1(a/l_1)K_0(R/l_1)}{l_1} \right.$$

$$+ D^{(3)}\frac{a \cdot I_1(a/l_2)K_1(R/l_2)}{l_2} \right]. \quad (68)$$

The plots of the trace of strain and the magnitude of the polarization for a cylindrical inclusion are qualitatively very similar to those for a spherical inclusion and hence have not been presented.

VI. SUMMARY

In summary, we discuss a theoretical framework that allows us to phenomenologically describe the observation of size-dependent electromechanical coupling due to strain or polarization gradients for nonpiezoelectric dielectrics. In such a "flexoelectric medium," we have derived the Green's functions or fundamental solutions for the governing equations. Anticipating that purely elastic nonlocal size effects may also be important at the nanoscale, those too are incorporated in our framework.[49] Employing the developed Green's functions, we present the solutions to Eshelby's transforming inclusion problem and provide explicit analytical expressions for the spherical and cylindrical shape.

We anticipate several applications of the present work, such as in the study of buried quantum dots. High electric fields may penetrate well within nanosize inclusions or persist close to interfaces even for micron-sized ones. Thus, the former may indicate possible applications in band structure tuning of embedded lattice mismatched quantum dots. Although simple lattice dynamical models may be employed to evaluate flexoelectric properties,[28] a direct calculation using the Berry phase approach[50] is desirable especially for the technologically important semiconductor quantum dot materials.

ACKNOWLEDGMENTS

*Author to whom correspondence should be addressed. Electronic address: psharma@uh.edu

[1] J. F. Nye, *Physical Properties of Crystals: Their Representation by Tensors and Matrices* (Oxford University Press; New York, 1985).

[2] A. K. Tagantsev, Phys. Rev. B **34**, 5883 (1986).

[3] R. D. Mindlin, Int. J. Solids Struct. **4**, 637 (1968).

[4] This fact is evident of course from the size independency of classical mechanics, though it is not strictly true from a physical perspective. There is a size dependency to strain at the nanoscale but that does not influence the point we are trying to make here; i. e., even if strain was size independent, the strain gradient scales linearly with size.

[5] C. L. Bauer and W. A. Brantley, Mater. Sci. Eng. **5**, 295 (1970).

[6] J. P. Nowacki, Arch. Mech. **56**, 33 (2004).

[7] E. V. Bursian and N. N. Trunov, Fiz. Tverd. Tela (Leningrad) **16**, 1187 (1974);[Sov. Phys. Solid State **16**, 760 (1974)].

[8] G. Catalan, L. J. Sinnamon, and J. M. Gregg, J. Phys.: Condens. Matter **16**, 2253 (2004).

[9] R. D. Mindlin, Int. J. Solids Struct. **5**, 1197 (1969).

[10] T. Dumitrica, C. M. Landis, and B. I. Yakobson, Chem. Phys. Lett. **360**, 182 (2002).

[11] S. M. Nakhmanson, A. Calzolari, V. Meunier, J. Bernholc, and M. B. Nardelli, Phys. Rev. B **67**, 235406 (2003).

[12] A. S. Nowick and W. R. Heller, Philos. Mag., Suppl. **14**, 101 (1965).

[13] W. H. Robinson, A. J. Glover, and A. Wolfenden, Phys. Status Solidi A **48**, 155 (1978).

[14] R. W. Whitworth, Philos. Mag. **4**, 801 (1964).

[15] R. D. Mindlin, J. Appl. Math. Mech. **35**, 404 (1971).

[16] R. B. Meyer, Phys. Rev. Lett. **22**, 918 (1969).

[17] V. L. Indenbom, V. B. Loginov, and M. A. Osipov, Kristallografiya **28**, 1157 (1981).

[18] D. Schmidt, M. Schadt, and W. Helfrich, Z. Naturforsch. A **27A**, 277 (1972).

[19] Sh. M. Kogan, Fiz. Tverd. Tela (Leningrad) **5**, 2829 (1963); [Sov. Phys. Solid State **5**, 2069 (1964)].

[20] W. Ma and L. E. Cross, Appl. Phys. Lett. **78**, 2920 (2001).

[21] M. Marvan and A. Havranek, Solid State Commun. **101**, 493 (1997).

[22] W. Ma and L. E. Cross, Appl. Phys. Lett. **81**, 3440 (2002).

[23] W. Ma and L. E. Cross, Appl. Phys. Lett. **82**, 3923 (2003).

[24] W. Cochran and R. A. Cowley, Phys. Chem. Solids **23**, 447 (1962).

[25] B. J. Dick and A. W. Overhauser, Phys. Rev. **112**, 90 (1958).

[26] K. B. Tolpygo, Fiz. Tverd. Tela (Leningrad) **4**, 1297 (1962); Sov. Phys. Solid State **4**, 1297 (1963).

[27] A. Askar, P. C. Y. Lee, and A. S. Cakmak, Phys. Rev. B **1**, 3525 (1970).

[28] A. Askar, P. C. Y. Lee, and A. S. Cakmak, Int. J. Solids Struct. **7**, 523 (1971).

[29] A. Askar and P. C. Y. Lee, Phys. Rev. B **9**, 5291 (1974).

[30] J. P. Nowacki and P. G. Glockner, Int. J. Eng. Sci. **15**, 183 (1979).

[31] A. K. Tagantsev, Phase Transitions **35**, 119 (1991).

[32] G. A. Maugin, *Continuum Mechanics of Electromagnetic Solids* (North-Holland, Amsterdam, 1988).

[33] J. D. Eshelby, Proc. R. Soc. London, Ser. A **241**, 376 (1957).

[34] J. Singh, *Physics of Semiconductors and Their Heterostructures* (McGraw-Hill, New York, 1992).

[35] E. Pan, J. Appl. Phys. **91**, 3785 (2002).

[36] E. Pan, J. Appl. Phys. **91**, 6379 (2002).

[37] J. Y. Li and M. L. Dunn, Philos. Mag. A **77**, 1341 (1998).

[38] R. Maranganti and P. Sharma, *Handbook of Theoretical and Computational Nanotechnology*, edited by M. Reith and W. Schommers (Schommers, Chap. 118 2006).

[39] E. Sahin and S. Dost, Int. J. Eng. Sci. **26**, 1231 (1988).

[40] H. Kleinert, *Gauge Fields in Condensed Matter*, Vol. 2 (World Scientific, Singapore, 1989).

[41] X. Zhang and P. Sharma, Int. J. Solids Struct. **42**, 3833 (2005).

[42] X. Zhang and P. Sharma, Phys. Rev. B **72**, 195345–1 (2005).

[43] J. P. Nowacki and R. K. T. Hseih, Int. J. Eng. Sci. **24**, 1655 (1986).

[44] G. W. Gibbons and B. F. Whiting, Nature **291**, 636 (1981).

[45] Z. Q. Cheng and L. H. He, Int. J. Eng. Sci. **33**, 389 (1997).

[46] Z. Q. Cheng and L. H. He, Int. J. Eng. Sci. **35**, 659 (1997).

[47] Quite interestingly, in the context of small quantum dots, there is a belief that embedded inclusions under strain adopt similar elastic moduli as of their host matrix rather than their unstrained (bulklike) value. See Maranganti and Sharma (Ref. 38) and references therein for a discussion of this issue. In any case, these subtleties are irrelevant for obtaining rough estimates, which we intend in this paragraph.

[48] $a_{11} = 8.767 \times 10^{19}$ dyn cm^2/C^2, $b_{11} = 1.921 \times 10^4$ dyn cm^4/C^2, $c_{11} = 1.188 \times 10^{12}$ dyn/cm^2, $d_{11} = 1.304 \times 10^8$ dyn cm/C, $f_{11} = 2.483 \times 10^{-2}$ dyn cm/C, ν (Poisson's ratio)$= 0.31$, $b_{44} = 0.5255 \times 10^4$ dyn cm^4/C^2, $c_{44} = 0.325 \times 10^{12}$ dyn cm^2/C, $d_{44} = 0.356 \times 10^8$ dyn cm/C, $f_{44} = 0.679 \times 10^{-2}$ dyn cm/C, $l' = 2.25 \times 10^{-7}$ cm. NaCl and KCl are the only nonpiezoelectric materials for which the flexoelectric and the reverse flexoelectric coefficients are known. To provide order-of-magnitude values for GaAs in Sec. VI, the flexoelectric coefficients are estimated to be the dielectric constant multiplied with e/a—where a is the lattice parameter of GaAs. The reverse flexoelectric parameters are estimated by using a simple scaling of the constants in NaCl. GaAs is cubic anisotropic. Isotropic averages are used for the elastic constants.

[49] With a few exceptions, for most metals and crystalline materials, the purely elastic nonlocal length scales are very small ∼1–2 Å, thus showing size effects only at impossibly small sizes of ∼1 nm or so. For some materials such as GaAs or graphite, the characteristic length scale is larger and nanostructures in the size-range of 5–10 nm may exhibit nonlocal elastic effects. See a recent discussion by Zhang and Sharma (Ref. 41).

[50] R. Resta, *Berry Phase in Electronic Wavefunctions* (Troisième Cycle de la Physique en Suisse Romande, Année Academique 1995-96, 1996).